Unsteady simulations of mixed convection heat transfer in a 3D closed lid-driven cavity

Ali Khaleel Kareem[a], Shian Gao[a], Ahmed Qasim Ahmed[a]

[a] Department of Engineering, University of Leicester, Leicester LE1 7RH, United Kingdom
[b] Engineering Department, University of Thi-Qar, Nassiriya, Iraq

Unsteady mixed convection heat transfer in a 3D closed cavity with constant heat flux on the centre part of the bottom wall and isothermal sidewalls moving in the same vertical direction is investigated numerically in this research. The other remaining walls forming the geometry are kept stationary and adiabatic. This research is accomplished with different Reynolds number, Re = 5000, 10000, 15000 and 30000. Numerical methodology based on the finite volume method is utilized. The simulations and analysis have been carried out by evaluating the performance of two turbulence methods, Unsteady Reynolds-Averaged Navier-Stokes (URANS) and Large Eddy Simulation (LES), in terms of flow vectors, isotherm contours, turbulent kinetic energy, the average Nusselt number (Nu_{av}) and the local Nusselt (Nu_{local}) number along the hot part of the bottom wall. The results show that by increasing the Reynolds number leads to enhanced Nusselt number and turbulent kinetic energy of the fluid in the domain. Moreover, both LES and URANS solutions captured the existence of the two primary vortexes (clockwise and anticlockwise). However, the comparisons have demonstrated clearly the ability and accuracy of the LES method in predicting the secondary vortexes in the corners of the cavity.

Keywords: Lid-driven cavity, Mixed convection, Turbulent flow, Unsteady simulation, LES, URANS

1. Introduction

Both natural and forced convection heat transfer types in either an enclosure or a moving wall cavity have been investigated in many research works. A sizable amount of research interests has been addressed in the last decades on both types of convection heat transfer. The effect of combined forced convection with free or natural convection is defined as mixed convection, which can be found in many engineering applications. Controlling heat convection transfer by either increasing or decreasing heat convection has a number of benefits on saving energy, increasing the device life or increasing the

device safety. Shear-driven flow or lid-driven flow is one of the configurations that has a lot of industrial and engineering applications such as air conditioning systems, electronic devices cooling,

Nomenclature

A	aspect Ratio	W	dimensionless velocity component at z-direction
Au	gold		
C	Smagorinsky coefficient	l	length of the heat source (m)
C_P	specific heat at constant pressure (J/kg K)	x	distance along the x-coordinate
		X	distance along the non-dimensional x-coordinate (x/L)
CO_2	carbon dioxide		
CFL	Courant–Friedrichs–Lewy number	Y	distance along the non-dimensional y-coordinate (y/H)
E	dimensionless length of the heat source (l/L)	Z	distance along the non-dimensional z-coordinate (z/D)
FVM	finite volume method		
Gr	Grashof number ($g\beta\Delta TW^3/v^2$)	*Greek symbols*	
h	convective heat transfer coefficient (W/m^2K)	α	thermal diffusivity of the fluid (m^2/s)
Ha	Hartmann number	β	volumetric coefficient of thermal expansion (1/K)
k	turbulent kinetic energy (m^2/s^2)		
L	width of the cavity (m)	μ	dynamic viscosity of the fluid (Pa/s)
MHD	magnetohydrodynamics	v	kinematic viscosity of the fluid (m^2/s)
Nu	Nusselt number		
Pr	Prandtl number (v/α)	v_{sgs}	sub-grid scale (SGS) viscosity
q"	heat flux (W/m^2)	θ	dimensionless temperature
Ra	Rayleigh number (Gr Pr)	ρ	density of the fluid (kg/m^3)
Re	Reynolds number (U_0W/v)	ε	dissipation rate of turbulent kinetic energy (m^2/s^3)
Ri	Richardson number (Gr/Re^2)		
$\overline{S}_{ij}$	large-scale strain rate tensor for grid-filter	δ_{ij}	Kronecker's delta
T	temperature of the fluid (K)	$\overline{\Delta}$	grid-filter width
t	time	τ_{ij}	subgrid-scale (SGS) stress tensor
TiO_2	titanium dioxide		
u	velocity component at x-direction (m/s)	*Subscripts*	
		av	average value
U	dimensionless velocity component at x-direction	b	buoyancy
		C	value of cold temperature
U_0	lid velocity (m/s)	H	value of hot temperature
v	velocity component at y-direction (m/s)	s	source
		sgs	sub-grid scale
V	dimensionless velocity component at y-direction	t	turbulent

lubrication technologies, high-performance buildings insulations, crystal growth and oil extraction [1]. It is well known that the cavity configurations and fluid types have significant effects on the heat convection. There are many geometric shapes of enclosure or lid-driven cavity which had been studied in the past with different boundary conditions such as rectangular, circular and triangular.

The research of the heat convection in lid-driven cavity problems has been continually developed. Many studies were carried out recently to quantify the natural convection of laminar and steady flow in different shapes of cavities. A numerical study was completed by Wang, et al. [2] to determine a 2D natural convection of a square cavity with cooled right vertical wall. The left vertical wall was sinusoidally oscillated at the constant average temperature of the cavity with adiabatic horizontal

walls. The enclosure was filled by nanofluid, and the influence of the nanofluid volume fraction on heat transfer was the main research objective. The outcome shows that the heat transfer and the oscillating behaviours were influenced by nanoparticles. A 2D steady laminar natural convection heat transfer and flow patterns of a wavy wall cavity with volumetric heat sources were numerically studied by Oztop, et al. [3]. The enclosure has a cooled right wall and heated left wall, while the wavy horizontal walls were kept isolated. The internal and external Rayleigh numbers (Ra) and the amplitude of wavy walls were the effective non-dimensional parameters. It was found that changing the values of internal to external Ra and wavy walls spaces affects the heat transfer and flow patterns. Also, the heat transfer direction was fully dependent on the internal and external Ra. A 2D natural convection in an open cavity filled by Al_2O_3-H_2O was analysed numerically by Mahmoudi, et al. [4]. Non uniform thermal boundary condition of the cavity was presented as well as the uniform heat generation or absorption. It was proved that by increasing the Hartmann number (Ha) leads to reducing the heat transfer, while it was increased by augmenting the value of the Rayleigh number. At Ra between 10^3-10^5 and Ha = 30, it was found that nanofluid has more significant impact on heat generation than heat absorption. A free convection cooling of nanofluid within modified 2D L-shape cavity was studied numerically by Saidi and Karimi [5]. It was illustrated that nanofluid has more enhancement than just pure water. In addition, at the low Rayleigh number and large values of aspect ratio, the heat transfer coefficient was enhanced. Moreover, the application of cylindrical pins showed improvement on the heat transfer rate.

On the other hand, mixed convection heat transfer of unsteady laminar flow in different cavity shapes was achieved in several investigations as well. Ismael, et al. [6] conducted numerically a study of water mixed convection heat transfer in a 2D square enclosure with a partial slip. The top wall was cooled, while the bottom wall was heated. The remaining walls of the cavity were kept adiabatic. Studying the effects of the pertinent parameters such as the slip parameter, Richardson number (Ri) and the direction of sliding walls was the major aim. A magnetohydrodynamics (MHD) mixed convection of nanofluid in a 2D lid-driven square cavity that contains rotating cylinder was simulated numerically by Selimefendigil and Öztop [7]. The major aim was the investigation of the effects of the dimensionless parameters such as Hartmann number, Richardson number, rotational speed of the cylinder, and the concentration of the nanoparticles. It was proved that by increasing the Ri leads to an increment of heat transfer. However, by increasing the value of the Hartmann number leads to a reduction of heat transfer. Rotation of the cylinder has a considerable effect on the heat transfer enhancement. A 2D MHD mixed convection of heated top moving wall enclosure that has inner central circular cylinder and heaters was studied numerically by Ray and Chatterjee [8]. It was shown that at the large size of the heater, the thermal field mostly depends on the heat source. In addition, when magnetic field is ignored, Richardson number can increase the effects of the heat transfer rate and the bulk fluid temperature. Also, inner circular objects lead to remarkable increase in Nusselt number. A mixed convection heat transfer of 2D moving wall square enclosure with heat that comes from inner triangular heat source was studied numerically by Kalteh, et al. [9]. It was found that Ag nanoparticles offered the highest average Nusselt number and the lowest value was given by using TiO_2 nanoparticles. Nusselt number was also increased by incrementing the nanoparticles volume fraction, while increasing nanoparticles diameters lead to decreasing the average Nusselt number. Abu-Nada and Chamkha [10] investigated numerically a 2D mixed convection nanofluid flow in an enclosure with moving top wall and wavy bottom wall. It was proved that at the considered Ri, the

nanoparticles have a significant effect on the heat transfer enhancement as well as the wavy bottom wall geometry ratios. Khanafer [11] compared numerically 2D steady laminar mixed convection heat transfer and flow performance in a top moving wall square cavity among different types of heated bottom wall conditions, including flat, flexible, rectangular and sinusoidal wavy walls. The results showed that at Re < 400 and Ri = 10^4, the flexible bottom wall can enhance the heat transfer by about 61.4% compared with flat and wavy bottom walls. While, by increasing Ri leads to reducing the heat transfer percentage of the flexible bottom wall and increasing the heat transfer for the rectangular wavy bottom wall.

The majority of numerical investigations is restricted to the two-dimensional geometry and only very limited work has been done on 3D lid-driven cavity problems [12-14]. A steady state natural convection and conduction heat transfer of H_2O-Au in a cubic cavity was investigated numerically by Ternik [13]. It was concluded that by increasing the volume fraction of nanoparticles at the same Rayleigh number value of the base fluid leads to decreasing the Ra number of the nanofluid. In addition, nanoparticles concentration has a major effect on the heat transfer. Investigation of natural convection heat loss control in a 3D solar cavity receiver containing inner plate fins was carried out numerically by Ngo, et al. [12]. It was observed that by using plate fins can lead to significant reduction in the natural heat convection.

Moreover, only limited attention has been paid to the study of the turbulent flow by using advanced models such as LES [14] or URANS [15-19]. Sharma, et al. [19] investigated numerically a 2D turbulent free convection in a closed cavity that was heated from the centre of the bottom wall and has a cooled sidewalls and adiabatic other walls. The standard k-ε model was utilized to model the turbulent natural convection. It was found that Nusselt number increases with incrementing the width of the heat source in the case of isotherm heating, while, in the case of isoflux heating, Nusselt number decreases with decreasing the heat source width. A double diffusive turbulent natural convection in a 2D closed square enclosure, filled by air and contaminant of CO_2, was investigated numerically by Serrano-Arellano, et al. [18]. It was observed that the location of CO_2 has considerable effects on the heat transfer in the closed cavity. In addition, the highest value of Nusselt number was found at the highest value of Rayleigh number with CO_2 that was located close to the heat source. Ridouane, et al. [17] numerically studied the features of the turbulent free convection of a 2D triangular cavity that is filled by air. The bottom wall of the enclosure was heated while the side walls were cooled. This kind of geometry can be found in conventional attic spaces of houses or buildings that have pitched roofs and horizontal suspended ceilings. It was concluded that this kind of geometry gains high turbulence level compared with square enclosure at given values of Rayleigh number. Cajas and Treviño [15] numerically analysed a 2D large aspect ratio enclosure. It was proved that at low values of Rayleigh number, there was no effect on the heat transfer instability, while there was an effect on the heat transfer at high values of Rayleigh number. Goodarzi, et al. [16] numerically analysed both laminar and turbulent mixed convection heat transfer of nanofluids inside a 2D shallow enclosure. It was observed that by increasing nanoparticles fraction leads to enhancing the heat transfer rate. In addition, turbulent kinetic energy, turbulence intensity, wall shear stress and skin friction were all affected by the nanoparticles concentration as well.

The above presented literature survey discussed various aspects of heat convection in different cavities. So it is not difficult to conclude that the majority of numerical investigations so far is restricted to two-dimensional geometry and only very limited investigations have been achieved on 3D

lid-driven cavity problems. Furthermore, too little attention has been paid to studying the turbulent flow by using an advanced turbulence method such as LES or URANS, and to analysing the heat convection and flow patterns in details. This paper aims to undertake a comprehensive evaluation and comparison for the ability and accuracy of URANS and LES methods, by detailed analysis of the flow patterns and temperature distributions of mixed convection heat transfer in a 3D two-sides lid-driven enclosure with different values of Reynolds number.

2. Methodology

The techniques of Computational Fluid Dynamics (CFD) are used in this project to simulate the flow and heat transfer characteristics in the cubic lid-driven enclosure. The governing equations are discretized in three-dimension by using the finite volume method (FVM), and the pressure-velocity coupling equations are solved by the SIMPLE algorithm. The convection terms in momentum and energy equations are discretized by using the QUICK scheme, and the implicit second order scheme is used for the time evaluation terms. The simulations are completed by using the commercial code ANSYS©FLUENT (version R15.0) [20].

2.1 Physical model

The main cubic geometry parameters are sketched in Fig. 1. The sidewalls of the enclosure are moving downward with a uniform velocity and are fixed at the cold temperature. The center part of the bottom wall (l) is heated at a constant heat flux, while the rest parts of the bottom wall and the top wall of the cavity are adiabatic. As it is mentioned previously, this kind of study can represent practical applications such as air cooling of the electronic devices. In this case, the moving sidewalls refer to the cold airflow along the cavity sides that are blown downwards by the effects of the fan or jet from the cavity top. The flow in the enclosure is a result of movement of the sidewalls and heat source at the bottom.
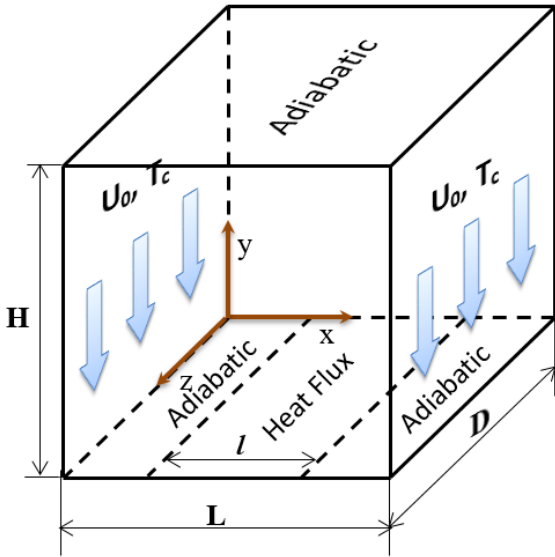
Fig. 1. Schematic diagram of cubic lid-driven cavity

The boundary conditions for the present problem are specified as follows:

Top wall: $\partial\theta/\partial Y = 0$, $U = V = W = 0$

Bottom wall: $\dfrac{\partial\theta}{\partial Y} = \begin{cases} 0, & \text{for } 0 < X < (1 - E)/2 \\ -1, & \text{for } (1 - E)/2 \leq X \leq (1 + E)/2 \\ 0, & \text{for } (1 + E)/2 < X < 1 \end{cases}$

Right and left walls: $\theta = 0$, $U = 0$, $V = -1$, $W = 0$

The condition $\partial\theta/\partial Y = -1$ for $(1 - E)/2 \leq X \leq (1 + E)/2$ at the bottom wall arises as a consequence of constant heat flux, q".

where θ is the dimensionless temperature.

The local Nusselt number and the average Nusselt number can be obtained respectively as:

$$Nu_{Local} = \frac{h_x}{k} = \frac{1}{\theta_s(X)} \tag{1}$$

$$Nu_{av} = \frac{\overline{h}}{k} = \frac{1}{E}\int_0^E \frac{1}{\theta_s(X)}\, dX \tag{2}$$

where $\theta_s(X)$ refers to the local dimensionless temperature, and h_x and $\overline{h}$ are the heat transfer coefficient on x-axis and the average heat transfer coefficient, respectively.

2.2 Governing equations

It is necessary to list the governing equations to complete the CFD models of the cubic lid-driven enclosure. Based on White [21] and Versteeg and Malalasekera [22], the continuity, momentum and energy equations can be written below for three dimensional flow of turbulence and an incompressible Newtonian fluid.

Continuity equation:

$$\frac{\partial\rho}{\partial t} + \frac{\partial u_i}{\partial x_i} = 0 \tag{3}$$

Momentum equation:

6

$$\frac{\partial u_i}{\partial t} + \frac{\partial (u_j u_i)}{\partial x_j} = -\frac{\partial P}{\partial x_i} + \frac{1}{Re}\left(\frac{\partial^2 u_i}{\partial x_i \partial x_i}\right) + \frac{Gr}{Re^2}\theta \tag{4}$$

Energy equation:

$$\frac{\partial(\theta)}{\partial t} + \frac{\partial(u_j\theta)}{\partial x_i} + \frac{1}{RePr}\left(\frac{\partial^2 \theta}{\partial x_i \partial x_i}\right) \tag{5}$$

Standard k-ε turbulence model:

The turbulent kinetic energy (k) and the dissipation rate (ε) are written in Cartesian coordinates (*i, j, k*) as shown below in equations (6) and (7) respectively [23].

$$\frac{\partial}{\partial t}(\rho k) + \frac{\partial}{\partial x_i}(\rho k u_i) = \frac{\partial}{\partial x_j}\left[\left(\mu + \frac{\mu_t}{\sigma_k}\right)\frac{\partial k}{\partial x_j}\right] + P_k + P_b - \rho\varepsilon + S_k \tag{6}$$

$$\frac{\partial}{\partial t}(\rho\varepsilon) + \frac{\partial}{\partial x_i}(\rho\varepsilon u_i) = \frac{\partial}{\partial x_j}\left[\left(\mu + \frac{\mu_t}{\sigma_\varepsilon}\right)\frac{\partial k}{\partial x_j}\right] + C_{1\varepsilon}\frac{\epsilon}{k}(P_k + C_{3\varepsilon}P_b) - C_{2\varepsilon}\rho\frac{\epsilon^2}{k} + S_\varepsilon \tag{7}$$

where S_k and S_ε refer to the user-defined source terms.

Turbulent viscosity is modelled as: $\mu_t = \rho C_\mu \dfrac{k^2}{\varepsilon}$ $\tag{8}$

Production of k: $P_k = -\overline{\rho u_i' u_j'}\dfrac{\partial u_j}{\partial x_i}$ $\tag{9}$

Effect of buoyancy: $P_b = \beta g_i \dfrac{\mu_t}{Pr_t}\dfrac{\partial T}{\partial x_i}$ $\tag{10}$

$C_{1\varepsilon}$, $C_{2\varepsilon}$ and $C_{3\varepsilon}$: model constants.

The sub-grid scale model of Smagorinsky-Lilly of LES approach is given by [24]:

$$\tau_{ij} - \frac{\delta_{ij}}{3}\tau_{kk} = -2\nu_{sgs}\bar{S}_{ij} = -2C\bar{\Delta}^2|\bar{S}|\bar{S}_{ij} = -2C\beta_{ij} \tag{11}$$

where

$$\beta_{ij} = -\bar{\Delta}^2|\bar{S}|\bar{S}_{ij} \tag{12}$$

$$\bar{S}_{ij} = \frac{1}{2}\left(\frac{\partial\bar{u}_i}{\partial x_j} + \frac{\partial\bar{u}_j}{\partial x_i}\right) \tag{13}$$

$$\bar{\Delta} = (\bar{\Delta}_x\bar{\Delta}_y\bar{\Delta}_z)^{\frac{1}{3}} \tag{14}$$

$$|\bar{S}| = (2\bar{S}_{ij}\bar{S}_{ij})^{\frac{1}{2}} \tag{15}$$

2.3 Code validation

Before starting any new numerical study, it needs to ensure that the numerical solver is validated thoroughly against the previous investigations. In this research, The first validation of the URANS modelling is completed against the results of Sharif [25] as shown in Fig. 2, for a laminar mixed convection flow in a top heated moving wall cavity filled with water at given Reynolds number. The second URANS validation, as shown in Fig. 3, is against the work of Chen and Cheng [26], who performed experimental and numerical laminar mixed convection heat transfer and flow pattern of air within an arc-shape cavity with cold moving top wall and heated stationary arc wall. Finally, as presented in Fig. 4, the LES predictions from the present study are validated against the experimental results by Prasad and Koseff [27]. Clearly, by looking at all three different cases that have been validated in this research, the present simulation results are found to agree very well with those from previous, which demonstrates that the current simulation methods are highly reliable and accurate.
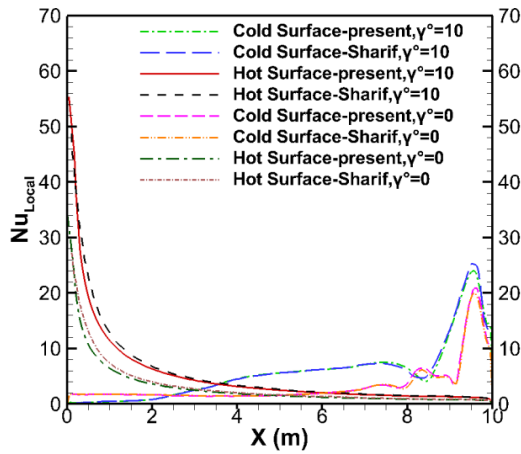
Fig. 2. Local Nusselt number comparison of present URANS modelling with Sharif [25].
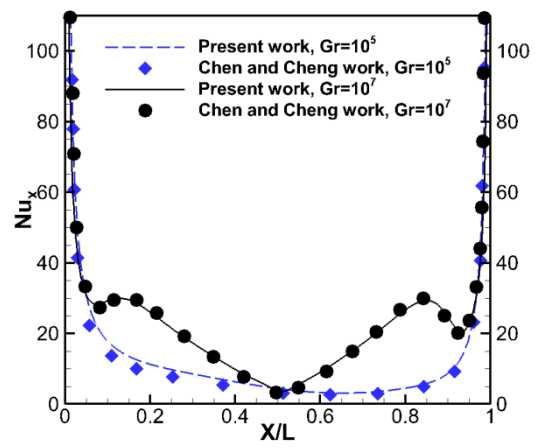
Fig. 3. Local Nusselt number comparison of present URANS modelling with Chen and Cheng [26].
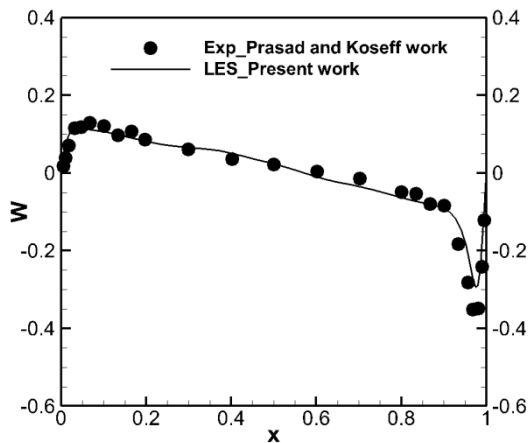
a) Left velocity
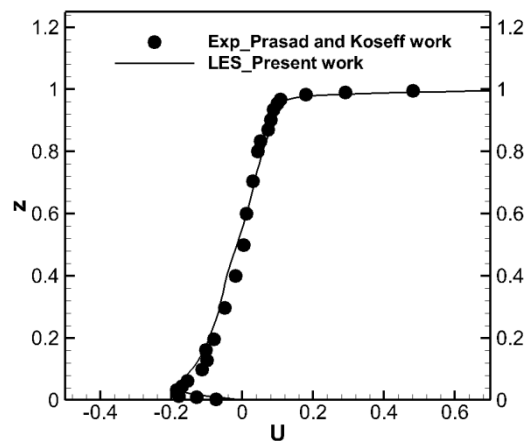
b) Right velocity

Fig. 4. Mean velocity profiles comparison of present LES work with Prasad and Koseff [27] at Re = 10000.

2.4 Grid independence tests

One of the main issues in CFD studies is grid independence tests, which is necessary in order to obtain the most suitable meshes for the cubic lid-driven enclosure. Discretising the domain is realized by structured and non-uniform meshes and the meshes close to the cubic walls are refined. The grid independence tests are carried out by using URANS approach with the standard k-ε model at constant values of Re = 5000, and A = 1. The convergence criteria are set as 10^{-6} for the discretized continuity, momentum and energy equations. Five different node numbers are tested in this model, which are 120000, 410625, 980000, 1699200 and 1921875, at Ri = 1 and non-dimensional time step is 0.0001, with the dimensionless wall distance, $y^{+} \approx 1$ and Courant–Friedrichs–Lewy number, CFL ≈ 0.3. As illustrated in Fig. 5, although there is not any big difference in the results by employing node number either equal to or higher than 980000, the number of grid points used in this research is chosen as 1699200 to obtain accurate results and to reach the grid independence.
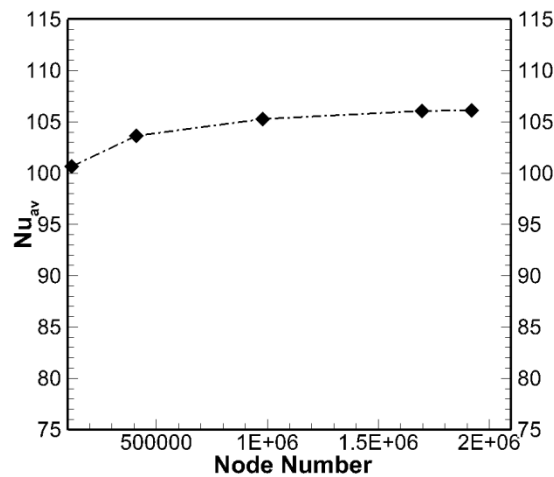
Fig. 5. Convergence of the average Nusselt number with grid refinement.

3. Results and discussion

The computed mixed convection flow and heat transfer in three dimensional CFD cases are examined in this section. Two different turbulent models are utilized, which are unsteady RANS and LES models. The outcomes are presented in terms of Nusselt number, isotherms contours, turbulent kinetic energy contours and velocity vectors by using both turbulent models.

3.1 URANS model

Fig. 6 outlines the local Nusselt number curves for the given four values of Reynolds number, Re= 5000, 10000, 15000 and 30000, at the midlines of the heated part of the bottom wall to investigate the influence of Reynolds number on heat transfer by using unsteady RANS model. The Standard k-ε turbulence model with time dependence is used in this test. Basically, the curves illustrate that increasing Re values lead to a significant enhancement in the local Nusselt number, which is mainly the consequences of increment in the velocity with higher Re number. Since higher movement of the fluid near the side walls is caused by the moving walls besides the temperature differences, it can be

seen that the local Nusselt number near the sides of the geometry is higher than that in the middle. The distributions of the local Nusselt number are symmetric about the midlines because of the symmetric boundaries of the current case.
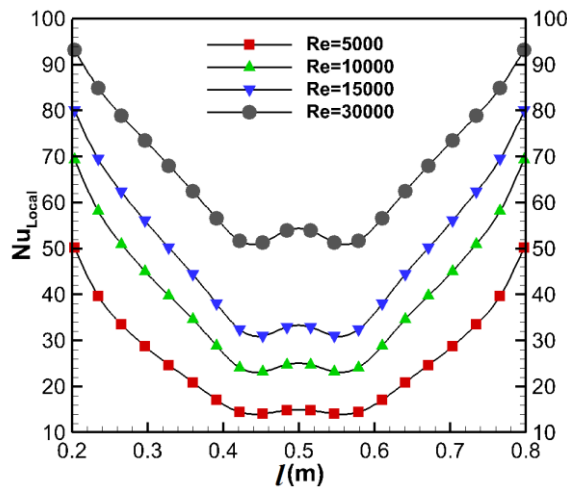
Fig. 6. Local Nusselt number distributions for different Reynolds numbers.

The turbulent kinetic energy is plotted in Fig. 7 for different Reynolds numbers at the horizontal midlines of the bottom wall, z = 0.5. The calculated values indicate that augmented value of Re leads to the enhancement in the fluctuation kinetic energy, which is the reason of increasing the value of fluid velocity within the enclosure and increasing the value of Grashof number. In addition, the turbulent kinetic energy rises gradually by increasing the Re, especially in the lid-driven areas. That is because of the higher turbulent velocity in these regions.
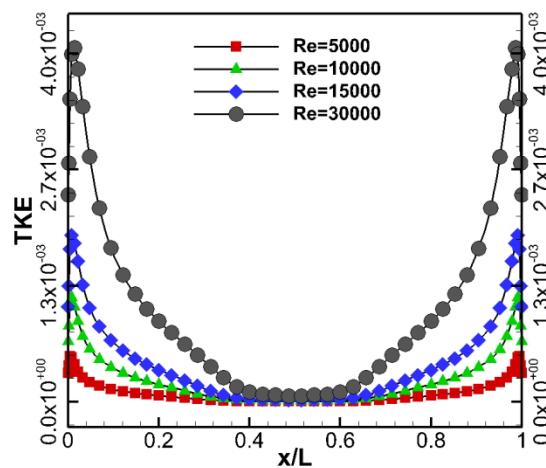
Fig. 7. Turbulent kinetic energy distributions for different Reynolds numbers.

3.2 Comparison between URANS and LES

In this section comprehensive comparison and explanation of the results, that originated from simulating unsteady turbulent flow of mixed convection heat transfer in the two-sides moving walls cavity by involving both the Smagorinsky LES model and standard k-ε of URANS model, are presented for two Reynolds numbers, Re = 5000 and 10000. Two different plane locations have been selected to get better understanding about the velocity and temperature field distributions. The outcomes and comparisons are completed in terms of velocity vectors, isotherms and Nusselt numbers. To make sure the LES simulations are well resolved, the power spectral density of the turbulence kinetic energy is shown in Fig. 8. It can be seen that the slope of -5/3 is observed visibly in the inertial subrange, which is known to represent the generic feature of turbulent flow. Therefore, the current simulation can be regarded as possessing the characteristics of a fully turbulent flow.
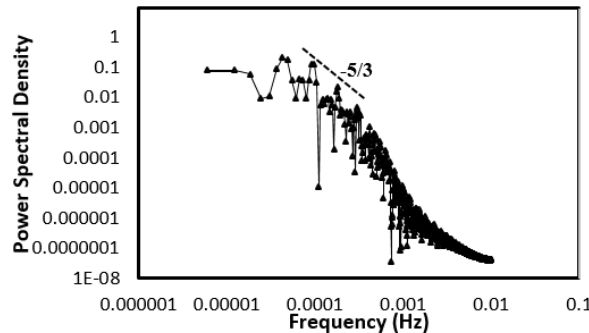
Fig. 8. Power spectral density of the turbulence kinetic energy.

3.2.1 Velocity vectors

The numerical results between URANS and LES in terms of flow vectors have been compared in this section. For the selected Reynolds number, Re=5000 and 10000, the velocity vectors in fully developed regions of the three dimensional flow are discussed here. Fig. 9a illustrates the flow behaviour for the x-y plane located at the middle of z-axis, while Fig. 9b deals with the y-z plane located at the midway of x-axis. Since the current case represents a symmetric domain, it can be noticed clearly that the flow structure is divided into two symmetric flow parts. Basically, it can be seen that the effects of forced convection due to the moving sidewalls are dominating, especially for the layers close to the moving walls. The flow thereabout the moving-walls is dragged due to shear and impinges onto the stationary-walls. With more details, at the corners of the domain, the flow deflects in the horizontal direction. The two primary vortexes (rotating clockwise and anticlockwise) nearby the domain centre are distinctly seen in Fig. 9a, and these vortexes are controlling the flow patterns by using either URANS or LES. Furthermore, the shown vectors in Fig. 9a and 9b plainly detect the existence of secondary eddies nearby the top corners and bottom centre, especially from the LES results, which are known as downstream and upstream secondary eddies. Lower secondary eddies are also revealed on the sides of the bottom wall. However, it can be seen obviously that the secondary eddies are shown more clearly by using LES approach for both selected planes and Reynolds numbers. Furthermore, increasing Reynolds number to 10000 it shows the ability differences between the two models in dealing with turbulent flow. The effect of changing the Reynolds number on the flow pattern is rather limited by using URANS, unlike the LES approach, which is able to show clearly the subaltern eddies.

11

Re=5000

Re=10000
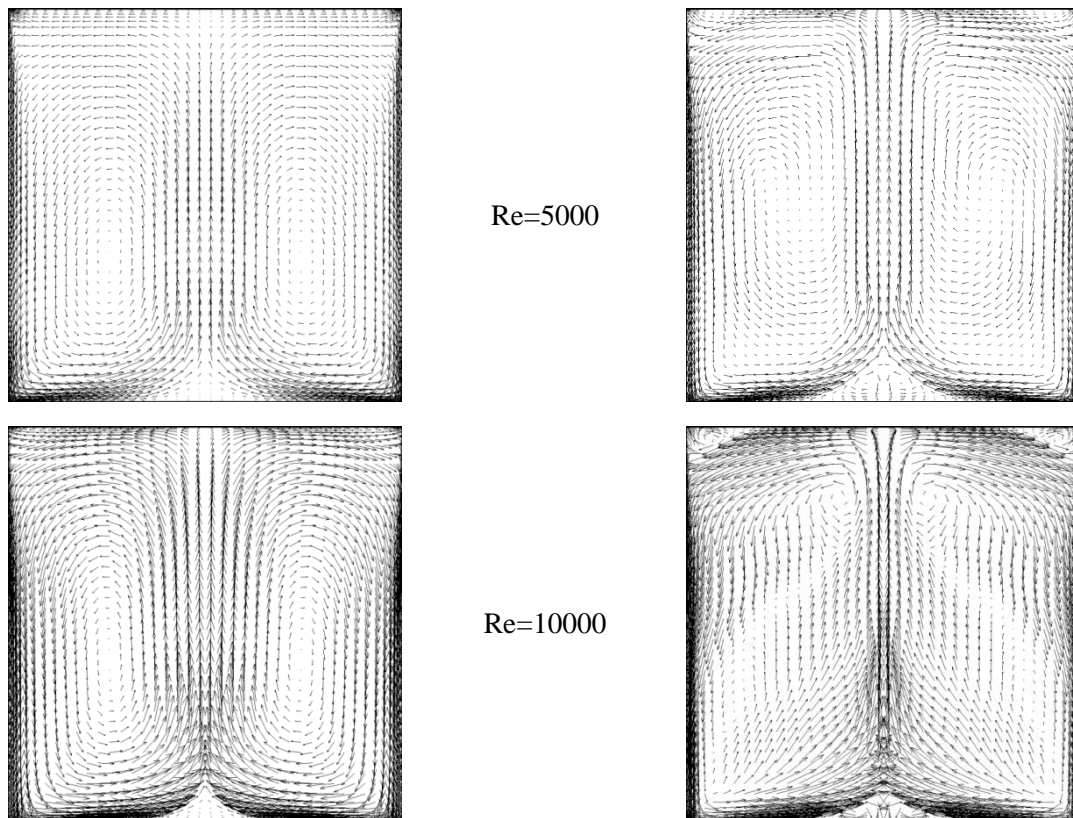
a) x-y plane located at the middle of z-axis

Re=5000

Re=10000
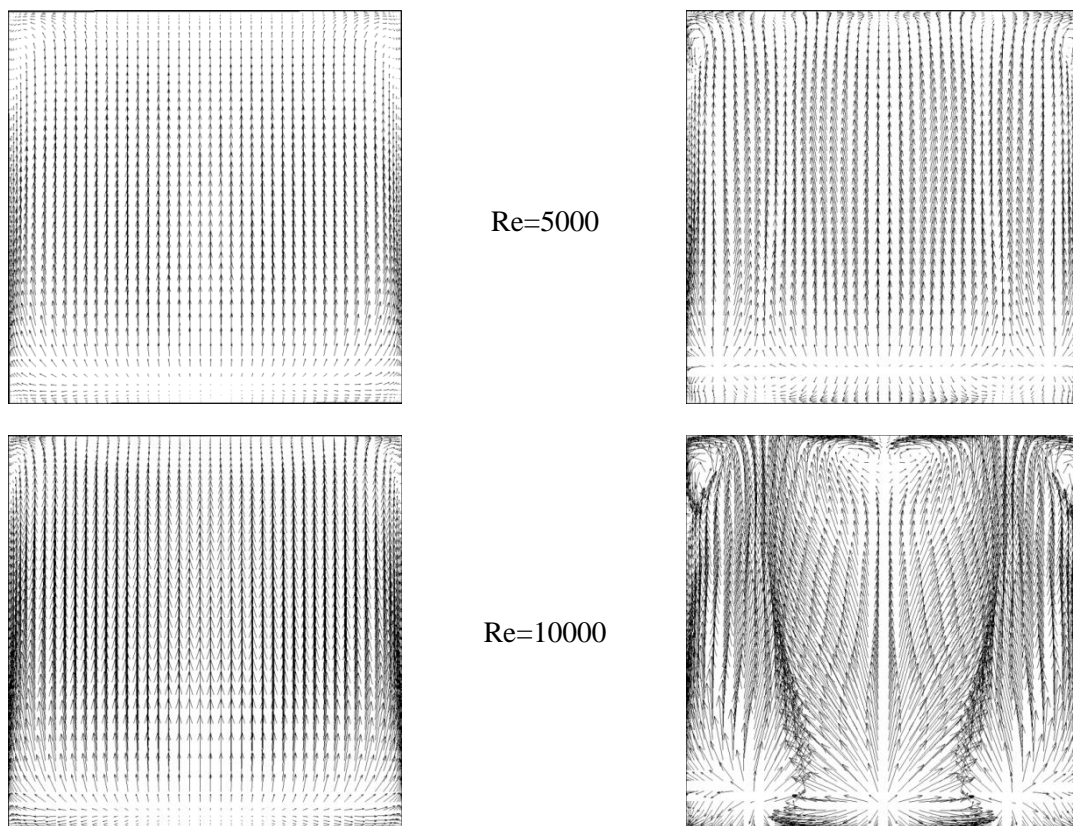
b) y-z plane located at the middle of x-axis

Fig. 9. Flow vectors comparison between URANS (left) and LES (right).

3.2.2 Instantaneous temperature field

URANS and LES predictions are compared in this section for the instantaneous temperature distributions at the selected Reynolds number, Re = 5000, for two different plane locations. Fig. 10 demonstrates the snapshots of instantaneous temperature patterns of the x-y plane located at the midway of z-axis by using LES and URANS. Fig. 10a presents the temperature contours at t = 10 sec. Hither it can be recognized that the URANS method predicted a semi-laminar plume rising from the heat source, while the LES method predicted the two primary vortexes (clockwise and anticlockwise) rising from the heat source area. At t = 16 sec, it can be observed that URANS started showing the vortex at the middle of the cavity and the upper part of the domain in thermally stratified state, whereas, the two primary vortexes predicted by the LES method keep expanding. At t = 28 sec, the first two symmetric vortexes (clockwise and anticlockwise) appear by harnessing URANS thereabout the sides of the bottom wall, however, by using the LES approach, apart from the two primary vortexes, two secondary eddies are shown nearby the sides of the bottom wall, and two small secondary eddies appear on the heated part of the bottom wall and at the corners of the top wall.

Moreover, Fig. 11 exhibits the snapshots of instantaneous temperature distributions of the y-z plane located at the centre line of x-axis. It demonstrates that from the beginning the URANS method provides thermally stratified isotherms that are almost parallel in the horizontal direction, except for the areas close to the moving walls. These parallel lines keep their shapes until covering the entire cavity. On the other hand, the LES predictions show clear differences in comparison to the URANS method. This is particularly observed that at t = 28 sec, multi-vortexes have formed, and they keep developing until covering the whole domain.

Furthermore, it can be observed from the temperature snapshots that the heat transfer thereabout the heat source is dominated by the natural convection. However, this domination is dwindling gradually by moving forward to the centre and the sides of the domain as the forced convection due to the moving sidewalls is controlling the mechanism of heat transfer in the cavity.

By taking other factors into account, URANS needed less computation time (22sec) to reach the fully developed state, whereas, LES needed 28sec. In comparison, it can be seen obviously from the temperature snapshots that LES can predict more flow details in the cavity, and both the temperature and the velocity vector distributions are more realistic.
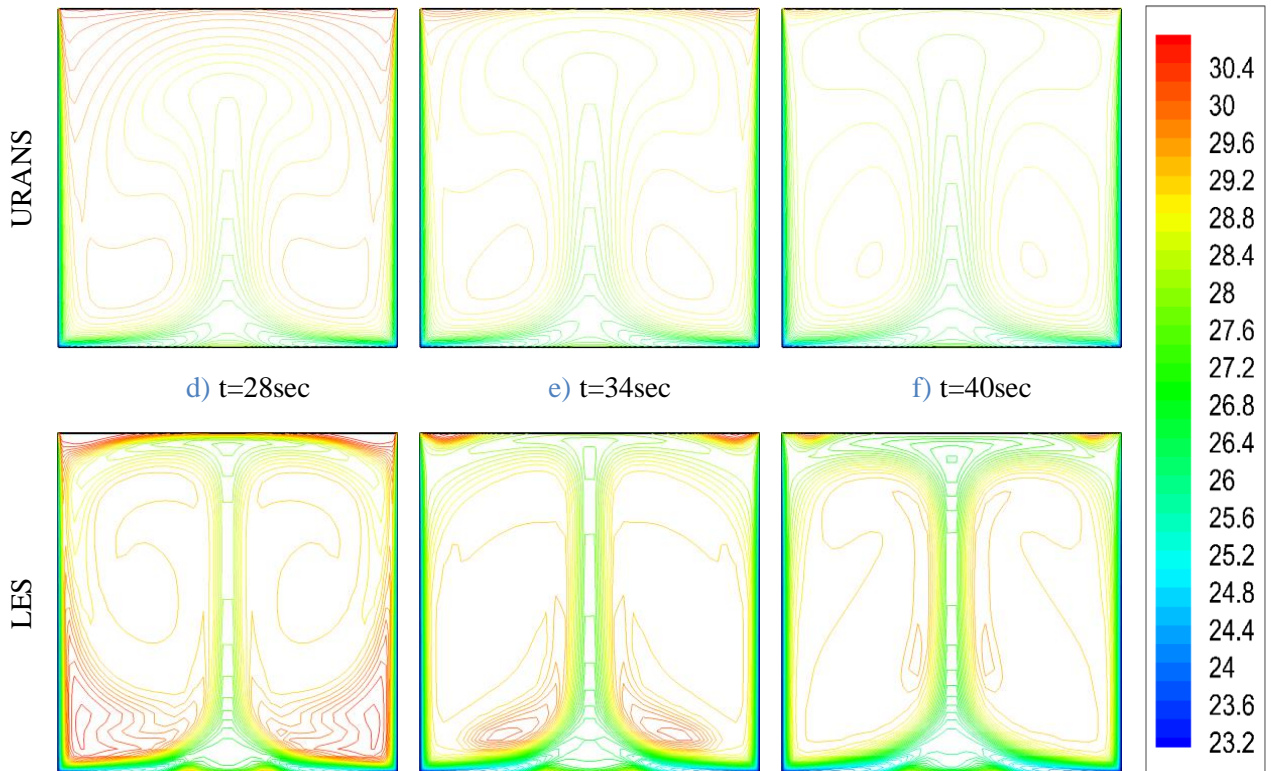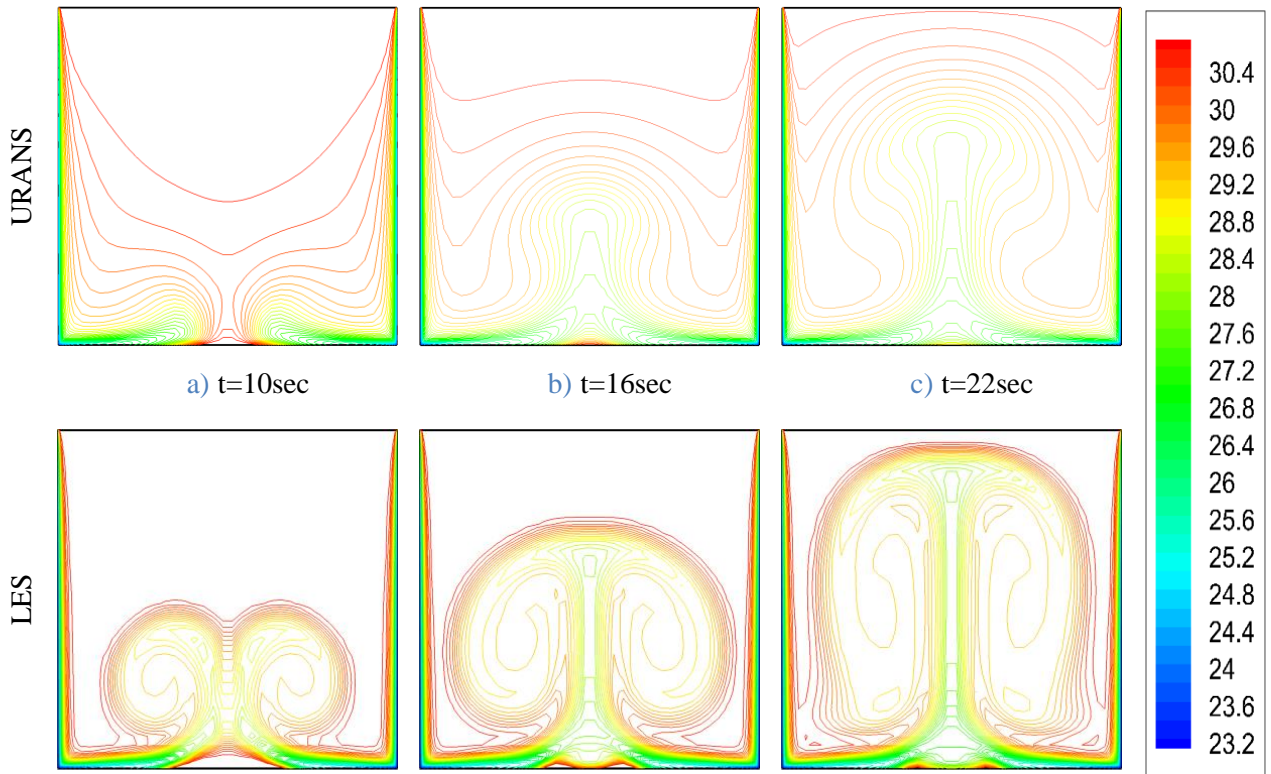
Fig. 10. Instantaneous isotherm comparison between URANS and LES for the x-y plane located at the middle of z-axis, at Re = 5000.
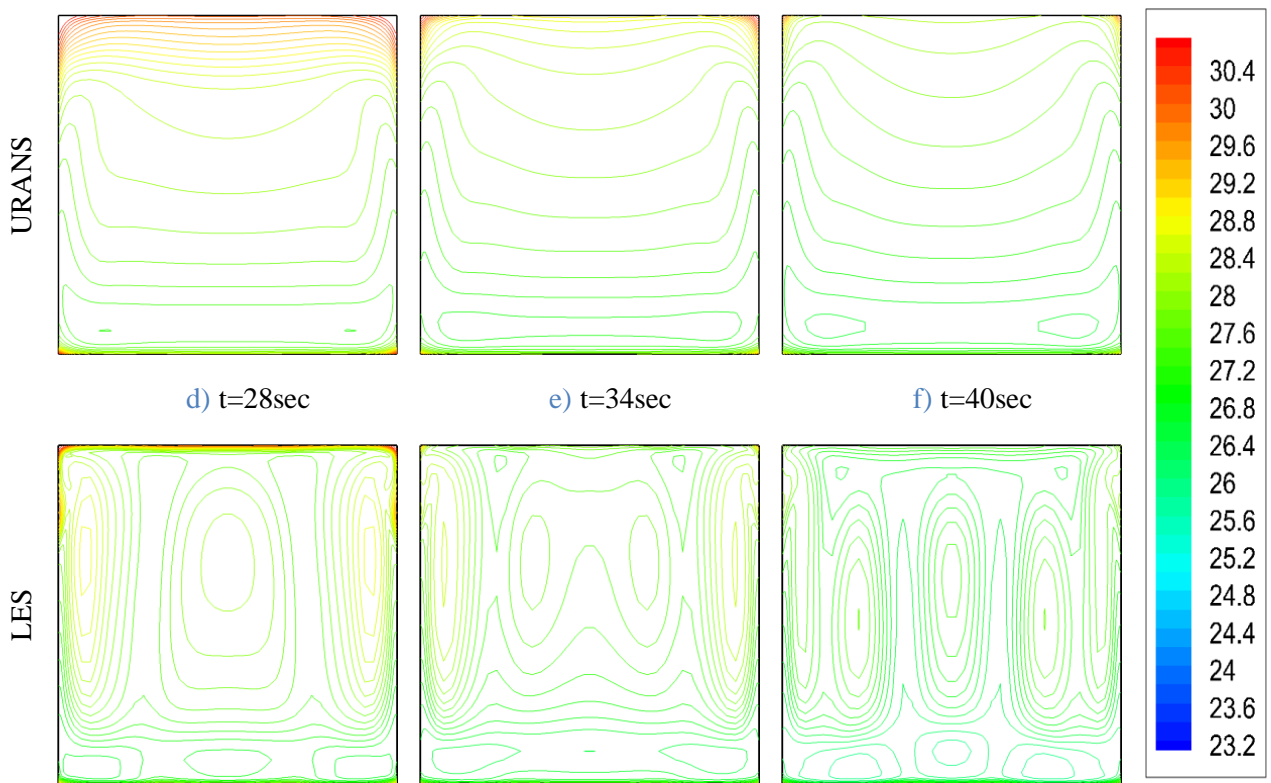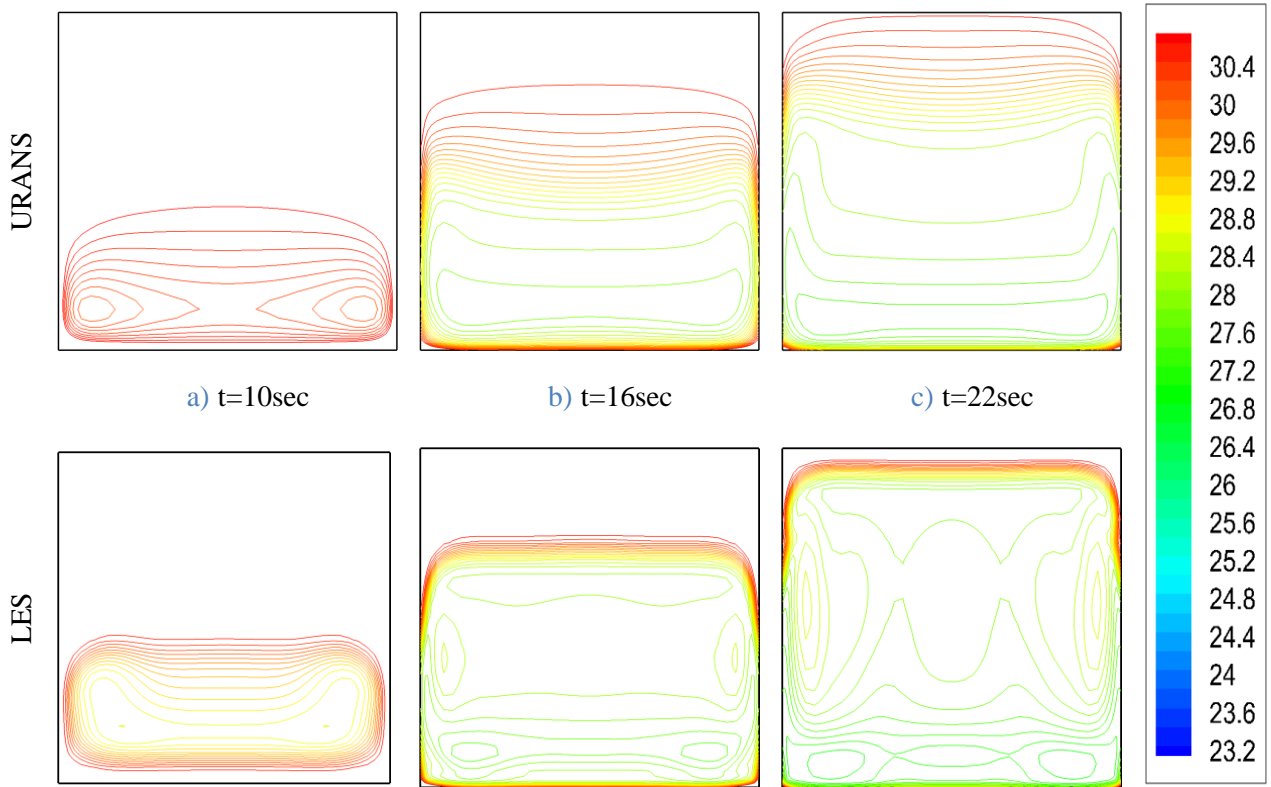
Fig. 11. Instantaneous isotherm comparison between URANS and LES for the y-z plane located at the middle of x-axis, at Re = 5000.

3.2.3 Average Nusselt number

Fig. 12 shows the comparison results of two turbulent methods in terms of average Nusselt number for three high values of Reynolds number. In general, it indicated that enhancement in the average Nusselt number can be achieved by increasing the Reynolds number with constant Grashof number. Furthermore, it can be observed that the LES method predicts slightly higher average Nusselt numbers, compared to the ones calculates by utilizing the URANS method.
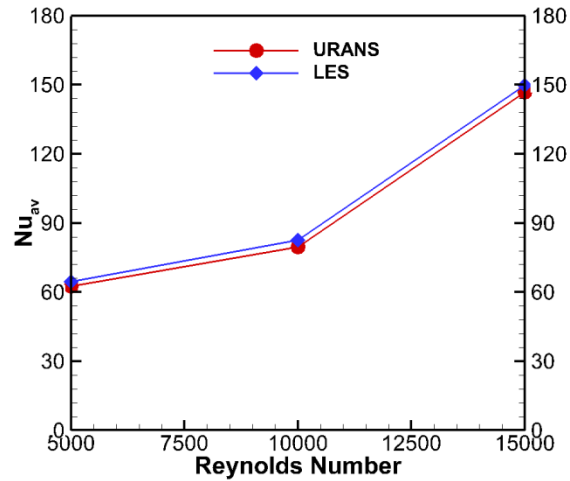
Fig. 12. Comparison of average Nusselt numbers for different Reynolds number.

4. Conclusions

The current paper addressed a three dimensional mixed convection heat transfer of water within closed lid-driven cavity that is heated partially at the bottom wall and has driven sidewalls. Interesting behaviours of URANS and LES models with varying Reynolds numbers are investigated. The current obtained results have revealed that:

- At constant Grashof number, increasing Reynolds number leads to augmentation in the average Nusselt number.
- The highest local Nusselt number occurs at the edges of the heat source surface while the lowest local Nusselt number occurs at the centre of the heat source.
- Reynolds number has a considerable effect on the flow structure and the turbulent kinetic energy, especially with the high speed regimes near the moving sidewalls of the enclosure.
- The flow structures in most areas of the cavity have been driven by the forced convection, except the area near the heat source is mostly controlled by the natural convection.
- At fully developed state, two main symmetric vortexes, clockwise and anticlockwise, are covering most of the cavity, while secondary eddies have been predicted at the corners of the cavity, especially by the LES method.
- Even though the LES approach needs more computational time, this work has demonstrated that LES has noticeable advantage over the URANS modelling in predicting accurate instantaneous temperature and velocity fields.

16

References

[1] H.M. Elshehabey, F. Hady, S.E. Ahmed, R. Mohamed, Numerical investigation for natural convection of a nanofluid in an inclined L-shaped cavity in the presence of an inclined magnetic field, International Communications in Heat and Mass Transfer, 57 (2014) 228-238.

[2] G. Wang, X. Meng, M. Zeng, H. Ozoe, Q. Wang, Natural Convection Heat Transfer of Copper–Water Nanofluid in a Square Cavity With Time-Periodic Boundary Temperature, Heat Transfer Engineering, 35(6-8) (2014) 630-640.

[3] H.F. Oztop, E. Abu-Nada, Y. Varol, A. Chamkha, Natural convection in wavy enclosures with volumetric heat sources, International Journal of Thermal Sciences, 50(4) (2011) 502-514.

[4] A. Mahmoudi, I. Mejri, M.A. Abbassi, A. Omri, Analysis of MHD natural convection in a nanofluid-filled open cavity with non uniform boundary condition in the presence of uniform heat generation/absorption, Powder Technology, 269 (2015) 275-289.

[5] M. Saidi, G. Karimi, Free convection cooling in modified L-shape enclosures using copper–water nanofluid, Energy, (2014).

[6] M.A. Ismael, I. Pop, A.J. Chamkha, Mixed convection in a lid-driven square cavity with partial slip, International Journal of Thermal Sciences, 82 (2014) 47-61.

[7] F. Selimefendigil, H.F. Öztop, Numerical study of MHD mixed convection in a nanofluid filled lid driven square enclosure with a rotating cylinder, International Journal of Heat and Mass Transfer, 78 (2014) 741-754.

[8] S. Ray, D. Chatterjee, MHD mixed convection in a lid-driven cavity including heat conducting circular solid object and corner heaters with Joule heating, International Communications in Heat and Mass Transfer, 57 (2014) 200-207.

[9] M. Kalteh, K. Javaherdeh, T. Azarbarzin, Numerical solution of nanofluid mixed convection heat transfer in a lid-driven square cavity with a triangular heat source, Powder Technology, 253 (2014) 780-788.

[10] E. Abu-Nada, A.J. Chamkha, Mixed convection flow of a nanofluid in a lid-driven cavity with a wavy wall, International Communications in Heat and Mass Transfer, 57 (2014) 36-47.

[11] K. Khanafer, Comparison of flow and heat transfer characteristics in a lid-driven cavity between flexible and modified geometry of a heated bottom wall, International Journal of Heat and Mass Transfer, 78 (2014) 1032-1041.

[12] L. Ngo, T. Bello-Ochende, J. Meyer, Numerical modelling and optimisation of natural convection heat loss suppression in a solar cavity receiver with plate fins, Renewable Energy, 74 (2015) 95-105.

[13] P. Ternik, Conduction and convection heat transfer characteristics of water–Au nanofluid in a cubic enclosure with differentially heated side walls, International Journal of Heat and Mass Transfer, 80 (2015) 368-375.

[14] Z. Zhang, W. Chen, Z. Zhu, Y. Li, Numerical exploration of turbulent air natural-convection in a differentially heated square cavity at Ra= 5.33× 109, Heat and Mass Transfer, 50(12) (2014) 1737-1749.

[15] J. Cajas, C. Treviño, Transient heating and entropy generation of a fluid inside a large aspect ratio cavity, International Journal of Thermal Sciences, 64 (2013) 220-231.

[16] M. Goodarzi, M. Safaei, K. Vafai, G. Ahmadi, M. Dahari, S. Kazi, N. Jomhari, Investigation of nanofluid mixed convection in a shallow cavity using a two-phase mixture model, International Journal of Thermal Sciences, 75 (2014) 204-220.

[17] E.H. Ridouane, A. Campo, M. Hasnaoui, Turbulent natural convection in an air-filled isosceles triangular enclosure, International Journal of Heat and Fluid Flow, 27(3) (2006) 476-489.

[18] J. Serrano-Arellano, M. Gijón-Rivera, J. Riesco-Ávila, F. Elizalde-Blancas, Numerical study of the double diffusive convection phenomena in a closed cavity with internal CO₂ point sources, International Journal of Heat and Mass Transfer, 71 (2014) 664-674.

[19] A.K. Sharma, K. Velusamy, C. Balaji, Turbulent natural convection in an enclosure with localized heating from below, International Journal of Thermal Sciences, 46(12) (2007) 1232-1241.

[20] A. FLUENT, 15.0 Theory Guide, Ansys Inc, 5 (2013).

[21] F.M. White, Fluid mechanics, WCB, ed: McGraw-Hill, Boston, (1999).

[22] H.K. Versteeg, W. Malalasekera, An introduction to computational fluid dynamics: the finite volume method, Pearson Education, 2007.

[23] P. Huang, J. Bardina, T. Coakley, Turbulence Modeling Validation, Testing, and Development, NASA Technical Memorandum, 110446 (1997).

[24] J. Smagorinsky, General circulation experiments with the primitive equations: I. the basic experiment*, Monthly weather review, 91(3) (1963) 99-164.

[25] M. Sharif, Laminar mixed convection in shallow inclined driven cavities with hot moving lid on top and cooled from bottom, Applied thermal engineering, 27(5) (2007) 1036-1042.

[26] C.-L. Chen, C.-H. Cheng, Experimental and numerical study of mixed convection and flow pattern in a lid-driven arc-shape cavity, Heat and mass transfer, 41(1) (2004) 58-66.

[27] A.K. Prasad, J.R. Koseff, Reynolds number and end-wall effects on a lid-driven cavity flow, Physics of Fluids A: Fluid Dynamics (1989-1993), 1(2) (1989) 208-218.